Journal of Chromatography, 350 (1985) 1–13
Elsevier Science Publishers B.V., Amsterdam — Printed in The Netherlands

CHROM. 18 117

STRUCTURE PARAMETERS OF MOLECULES AND MEDIA EVALUATED BY CHROMATOGRAPHIC PARTITION

I. CONTROLLED-PORE GLASSES

HENRIK WALDMANN-MEYER
Fysisk-Kemisk Institut, Technical University of Denmark, DK 2800 Copenhagen-Lyngby (Denmark)
(Received June 25th, 1985)

SUMMARY

Polystyrene, dextran and sodium dodecyl sulphate–protein data for eleven controlled-pore glasses have been used to validate the expression $K_D = (b - R_e/R_x)^2$ derived from a geometrical exclusion model for cylindrical pores. The calculated pore radii (R_x) agreed well with mercury-intrusion values, and the crucial role of Stokes' radius (R_e) was confirmed by comparison with Casassa's formulations [E. F. Casassa and Y. Tagami, *Macromolecules*, 2 (1969) 14; E. F. Casassa, *J. Polym. Sci., Part B*, 5 (1967) 773]. From theory it was demonstrated that for any molecule, $R_e = A\,M^x$ where A and x are defined, structure-specific constants. Thus, linear $K_D(M)$ functions were derived and tested, by which one is able to distinguish between coils, rods and ellipsoids, ideal and real solvents, and to determine bond lengths, expansion, gyration radii, axial ratios and diffusion coefficients. The characteristic shape of the empirical K_D:log M curves derives directly from the linear $K_D(M)$ function.

INTRODUCTION

The mechanisms that give rise to chromatographic partition have been extensively investigated. There is now a consensus to regard partition as a diffusive quasi-equilibrium process, which depends on both size and shape of the permeating molecule as expressed by the effective hydrodynamic radius. However, very little is known about the effect of the pore or cavity conformation and size. Controlled-pore glasses (CPG) are the most adequate medium for studying this problem, since these glasses can be obtained with extremely narrow pore distributions, so that the pore radii can be measured with high precision by means of mercury-intrusion porosimetry.

Equations for the partition of random-flight polymer chains in rigid lamellar, spherical and cylindrical cavities have been formulated by Casassa and Tagami[1] and applied to literature data for chromatography in CPG.

On the other hand, on the basis of a simple geometrical exclusion model (GEM), equations for both glasses and gels have been derived[2–4] which take into account not only the shape of the pores or voids but also their size. In this paper the

0021-9673/85/$03.30

GEM theory will be elaborated and applied to literature data for random coiled and rod-like molecules analysed in CPG of eleven different pore sizes. The GEM correlation between partition coefficient and molecular radius will be tested with respect to the calculated pore size, its assumed shape, and the requirement of using the hydrodynamic radius. The results will be compared with those obtained by Casassa[5] from the same experimental data.

By combination with physicochemical rules for macromolecules, the equations are then extended to cover partition as a function of the molecular weight, for which no theory has so far been advanced. The specificity of this function will be described and substantiated by the experimental results. Moreover, it will be shown that fundamental structural and thermodynamic parameters can be determined from the linearized GEM plots, a fact that conveys unsuspected perspectives to exclusion chromatography.

THEORY

Partition as function of molecular radius and pore size

In the following it is assumed that the average pore conformation in CPG can be represented by straight cylinders. Tubular pores have in fact been directly observed by means of scanning electron micrography[1]. We further consider the pore diameter to be uniform, as it is the case with the glasses prepared by Haller[6,7] employed throughout the experiments described here.

Let V_e denote the elution volume, V_0 the extraporous solvent and V_i the intraporous volume as measured by eluting a small solute molecule or by weighings under the usual non-equilibrium conditions. For an assembly of N rigid cylindrical pores with an average length H and radius R_x, the measured pore volume is then

$$V_i = N \pi H R_x^2 \tag{1}$$

Since it is well established that small solvent molecules can diffuse into glass, the volume taken up by these molecules at equilibrium is larger than V_i, namely

$$V_i^* = V_i + V_m = N \pi H(R_x + \delta)^2 \equiv N \pi H(R^*)^2 \tag{2}$$

where V_m is the solid volume of the hollow cylinder constituting the intravitreous diffusion layer, δ its radius, and R^* denotes the overall pore radius $(R_x + \delta)$.

This implies that the volume available to the centre of mass of a solute molecule of radius R_e is, evidently, $N \pi H(R_x - R_e)^2$, and the liquid volume required to elute this molecule from the pores is

$$V_e - V_0 = N \pi H(R^* - R_e)^2 \tag{3}$$

where R_e is the effective hydrodynamic (Stokes') radius of a molecule. It is the basic parameter operative in all diffusion processes. Thus, for translational diffusion,

$$R_e = k_B T/(6 \pi \eta D^0) \tag{4}$$

with k_B denoting the Boltzmann constant, η the solvent viscosity and D^0 the diffusion coefficient at zero diffusant concentration.

In consequence, the measured partition coefficient, K_D, will slightly be larger than the real coefficient, K_D^*, since

$$K_D = \frac{V_e - V_0}{V_i} = K_D^* V_i^*/V_i = K_D^* (1 + V_m/V_i) = K_D^*(R^*/R_x)^2 \quad (5)$$

and from eqns. 1 and 3, K_D can be expressed as

$$K_D = \left(\frac{R^* - R_e}{R_x}\right)^2 \equiv \left(b - \frac{R_e}{R_x}\right)^2 \quad (6)$$

Thus, a correlation of $K_D^{\frac{1}{2}}$ *vs.* R_e gives a straight line with a slope of $-1/R_x$, an extrapolated ordinate intercept of $b = (R^*/R_x) > 1.00$ and an abscissa intercept at R^*.

We now let R_{Hg} denote the pore radius measured by means of mercury-intrusion porosimetry. Owing to interfacial tension, mercury molecules will not diffuse into glass, which implies that

$$R_x = R_{Hg} \quad (7)$$

The validity of this equation is the crucial test of the GEM theory for porous glass. In order to perform this test, the molecular parameters used in the literature data treated below have to be converted into R_e values before eqn. 6 is applied. If the identity $R_x = R_{Hg}$ is verified, the cylindrical pore shape is confirmed, as well as the fact that R_e is the basic parameter in exclusion processes. This implies that the correlation between K_D and the molecular weight must follow the $R_e(M)$ function for the particular chemical species.

Stokes' radius functions of the molecular weight

In this section it is shown that for any molecule large enough to follow Stokes' law, the radius can be expressed as

$$R_e = A M^x \quad (8)$$

and that x and A are structure-specific constants that reflect hydrodynamic structure, axial ratios, bond lengths, partial specific volume and molecular expansion. The theory for most of the derivations is covered by advanced textbooks[8–10].

Random coils. Random structures are evaluated statistically by means of the root-mean-square radius of gyration R_G or $\langle s^2 \rangle^{\frac{1}{2}}$, given by

$$R_G = \alpha \beta (M/6 M_0)^{\frac{1}{2}} \quad (9)$$

where α denotes a molecular expansion coefficient, β the effective monomer–monomer bond length and M_0 the monomer molecular weight. The Stokes' radius is obtained from

$$R_e \simeq \frac{0.6647\ R_G}{1 + 0.814\alpha/(M/M_0)^{\frac{1}{2}}} \tag{10}$$

which, for large values of M/M_0, yields

$$R_e \simeq 0.6647\ R_G \tag{10a}$$

From eqns. 10a and 9,

$$R_e \simeq A_\theta\ M^{\frac{1}{2}}\ \alpha \tag{11}$$

where $A_\theta \equiv 0.6647\beta/(6\ M_0)^{\frac{1}{2}}$ is constant for a given substance and temperature. The expansion coefficient α is unity in ideal solvents, *i.e.* poor solvents at $T = \theta$, and increases in real solutions with the molecular weight as $\alpha = \zeta M^z$, where $0 \leqslant \zeta \leqslant 1$ and $0 \leqslant z < \approx 0.1$. Thus

$$R_e \simeq A_\theta \cdot M^{\frac{1}{2}} \qquad (T = \theta) \tag{11a}$$

and

$$R_e \simeq A_\theta\ \zeta\ M^{\frac{1}{2}+z} \qquad (T \neq \theta) \tag{11b}$$

It is noted that, for polydisperse coils, M obtained from sedimentation and diffusion ($\bar{M}_{S,D}$) ought to be used in any correlation with R_e. A further correlation between radius and molecular weight is obtained from the intrinsic viscosity as

$$[\eta]MK' = R_\eta^3 = (R_e/\chi)^3 = (R_G\xi)^3 \tag{12}$$

with $K' \equiv 3/(10\ \pi\ N_A)$ and $[\eta]$ in units of cm^3/g. For high molecular weight, theory yields a ξ value of 0.875 whence, by eqn. 10, $\chi \simeq 0.76$. For ideal solutions a ξ value of 0.835 appears to be appropriate[8]. By substituting for R_G from eqn. 9, the Mark–Houwink expression $[\eta] = K''M^a = K''\ \alpha^3\ M^{\frac{1}{2}}$ is obtained.

Ellipsoids. The effective hydrodynamic radius is given by

$$R_e = (K\ \bar{V}_h\ M)^{1/3} \cdot f/f_0 \equiv A_0 M^{1/3}\ f/f_0 \tag{13}$$

K stands for $2.5\ K' = 3/(4\ \pi\ N_A)$, $\bar{V}_h$ is the partial specific volume including bound solvent, and the frictional ratio f/f_0 represents the deviation from spherical shape, from which the axial ratio a/b is readily computed. For a given range of a/b one finds that $f/f_0 = \mu(a/b)^m$ where μ and m are positive and become constant for high axial ratios. Hence

$$R_e = (K\ \bar{V}_h\ M)^{1/3}\ \mu(a/b)^m = A_0\ M^{1/3}\ \mu(a/b)^m \tag{14}$$

In the following, μ and m will specifically denote the coefficients applying to prolates.

Rods. Most equations for rod-like molecules of length L and diameter d are approximations valid for $L \gg d$. They cannot *a priori* be expected to apply to our data for proteins of $M \approx 18\,000$–$90\,000$ denaturated by sodium dodecyl sulphate (SDS). A general approach to transport properties of rods is to treat them as prolate ellipsoids of $a/b = (2/3)^{\frac{1}{2}}\, L/d$. In the case of SDS-treated proteins, it is sustained that SDS binds to most proteins on the same weight-per-weight basis, so that the length of the rod formed increases linearly with M. Hence, for $d \approx$ constant, $(a/b) \cdot p = M$, wherefrom by eqn. 14, for homologuous rods[11]

$$R_e = (K\, \bar{V}_h\, M)^{1/3}\, \mu(M/p)^m = A_0\, \mu\, p^{-m}\, M^{1/3+m} \tag{15}$$

When no diffusion data are available, R_e is evaluated from $[\eta]$ and M as follows. For rigid particles $[\eta] = \nu\, \bar{V}_h$, where the Simha shape factor ν evidently increases with M in the case of homologuous rods. On the other hand, a rod of length L can be approximated by L/d touching spheres of diameter d. This is essentially the Flory model for coils, from which $[\eta]$ is obtained as a function of M (*cf.* eqn. 12). Thus, by inserting $[\eta] = \nu\, \bar{V}_h$ into eqn. 12,

$$(R_e/\chi)^3 = R_\eta^3 = \nu\, \bar{V}_h\, M\, K' \tag{16}$$

and[11] by combination with eqn. 13, for rigid molecules

$$\chi = (2.5/\nu)^{1/3}\, f/f_0 \tag{17}$$

Therefore, χ is 1.00 for spheres, and decreases with increasing a/b as $(f/f_0)/\nu^{1/3}$ decreases. This means that a/b must be known to calculate R_e from R_η as obtained from eqn. 12.

By setting $\nu = \mu'(a/b)^{m'}$, which for homologous rods equals $\nu = \mu'(M/p)^{m'}$, it is readily seen that $[\eta] = \nu\, \bar{V}_h$ varies as $M^{m'}$ while R_η is proportional to $M^{(m'+1)/3}$. By means of m' an approximate value for the actual a/b range can be evaluated from log ν: log a/b. An average χ value applied to R_η will then result in rather accurate R_e values without the need of assumptions as to the size of $\bar{V}_h$.

Partition as a function of molecular weight

From the preceding, it is readily seen that data obtained from analysis in the same porous medium fall on the same curve when plotted as any function of K_D *vs.* $R_e \times$ a constant k. Thus $1/D^0$ or $M(1 - \bar{V}\rho)/s^0$ would apply to all structures, and R_η or $(M[\eta])^{1/3}$ to coils or rods. The latter is, in fact, the basis for Bénoit *et al.*'s 'universal calibration'[12]. By use of eqn. 6 a straight line is obtained in all cases, from which the pore radius R_x may be calculated, provided k is known.

In contrast, most valuable information is obtained by combining eqn. 6 with any of the expressions generalized as $R_e = A\, M^x$ (eqn. 8). Thus, for coils in a θ medium, from eqns. 6 and 11a

$$K_D^{\frac{1}{2}} = b - M^{\frac{1}{2}}\, A_\theta/R_x \tag{18}$$

whence the important bond length β can be calculated from the slope of a $K_D^{\frac{1}{2}}$ *vs.* $M^{\frac{1}{2}}$

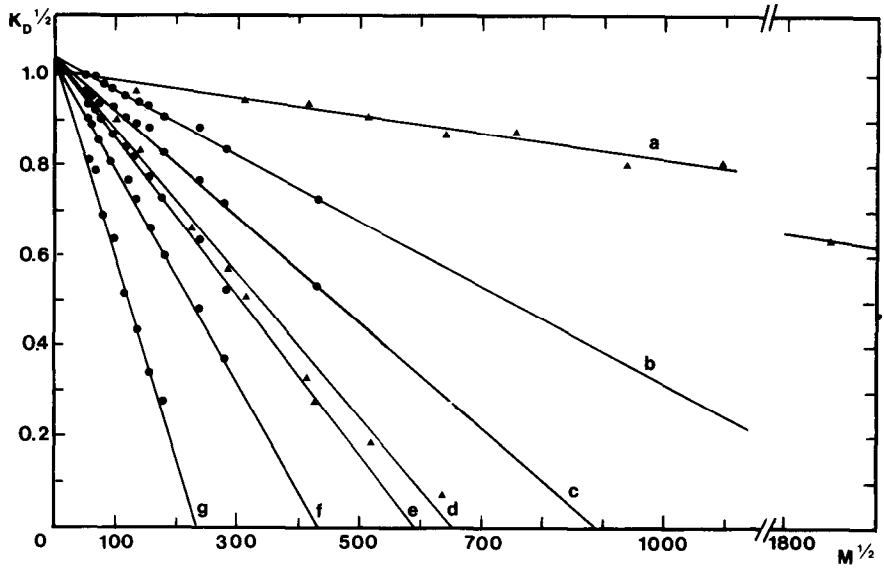

Fig. 1. Random coils in ideal solvents (eqn. 18) (*cf.* Table II). Polystyrenes (▲): (a) R_x 905; (d) R_x 113. Dextrans (●): (b) R_x 276; (c) R_x 173; (e) R_x 113; (f) R_x 85; (g) R_x 45.

plot (Fig. 1). If the exponent in the Mark–Houwink equation $[\eta] = K'' \zeta^3 M^{\frac{1}{2}+3z}$ is known, for coils in real solutions it is seen from eqn. 11b that

$$K_D^{\frac{1}{2}} = b - M^{\frac{1}{2}+z} \zeta A_\theta / R_x \tag{19}$$

In most cases, however, the exponent of M is not known *a priori*. Therefore, from eqns. 6 and 8 the GEM equation valid for all structures is given by

$$-\ln(b - K_D^{\frac{1}{2}}) = -x \ln M - \ln(A/R_x) \tag{20}$$

TABLE I

EVALUATION OF STRUCTURE PARAMETERS BY GEM EQUATIONS

R_x = Pore radius; $A_\theta = 0.2714\ \beta/M_0^{\frac{1}{2}}$, where β is the effective bond length, and M_0 is the monomer molecular weight; $A_0 = (K\bar{V}_h)^{1/3}$, where $K = 3/(4\pi N_A)$, and $\bar{V}_h$ is the partial specific volume including bound solvent; α(expansion factor) = ζM^z. f/f_0 (frictional ratio) = $\mu(a/b)^m = \mu(M/p)^m$, where a/b is the axial ratio of a prolate ellipsoid, and $p \equiv M/(a/b)$ for homologous rods; D^0 = diffusion coefficient; R_G = radius of gyration ($\langle s^2 \rangle^{\frac{1}{2}}$).

	Equation	*Slope*	*y-Intercept*	*Evaluation*
Coils	Eqn. 6	$-1/R_x$	b	R_x
	Eqn. 18	$-A_\theta/R_x$	b	β, R_G, D^0
	Eqn. 20, $T = \theta$	$-1/2$	$-\ln(A_\theta/R_x)$	β, ideality, R_G, D^0
	Eqn. 20, $T \neq \theta$	$-(1/2 + z)$	$-\ln(A_\theta\zeta/R_x)$	(α), R_G, D^0
Ellipsoids and rods	Eqn. 6	$-1/R_x$	b	R_x
	Eqn. 20	$-(1/3 + m)$	$-\ln[A_0\mu/(p^m R_x)]$	a/b, D^0 Globular *vs.* rod-like structure

This expression will be applied to experimental data for polystyrenes, dextrans and SDS-proteins in the following. An entirely analoguous equation has been formulated for gels[3].

Differing from the empirical K_D : log M plots, the linear GEM correlation is theoretically founded and permits the evaluation of fundamental molecular parameters as well as the distinction between different types of structure. These features are summarized in Table I. The determination of $b = R^*/R_x$ is discussed below.

MATERIALS AND DATA TREATMENT

Polystyrenes

The data were obtained by Moore and Arrington[13] in a polar θ solvent at 25°C on two different CP glasses provided by Haller. Twelve different samples were used, covering a $\bar{M}_w$ range from $3.5 \cdot 10^6$ to $1.05 \cdot 10^4$, with $(\bar{M}_w/\bar{M}_N) < 1.25$ for all but the lightest fraction. $\bar{M}_w$, R_G, V_e, V_0 and $V_i + V_0$ were tabulated. V_0 was evaluated by means of colloidal latex and $V_i + V_0$ by benzene. R_G *vs.* V_e plots were shown for both glasses.

We calculated R_e by means of eqn. 10, setting $\alpha = 1$ and $M_0 = 52$ g/mol, as each styrene ($M_0 = 104$) contains two C–C bonds[8]. The correlations according to eqns. 18 and 20 appear in Figs. 1 and 2, and the numerical results are given in Table II.

Dextrans

Fourteen dextran fractions, analysed by Basedow *et al.*[14] for $\bar{M}_w$, $\bar{M}_N$, $\bar{M}_z$ and

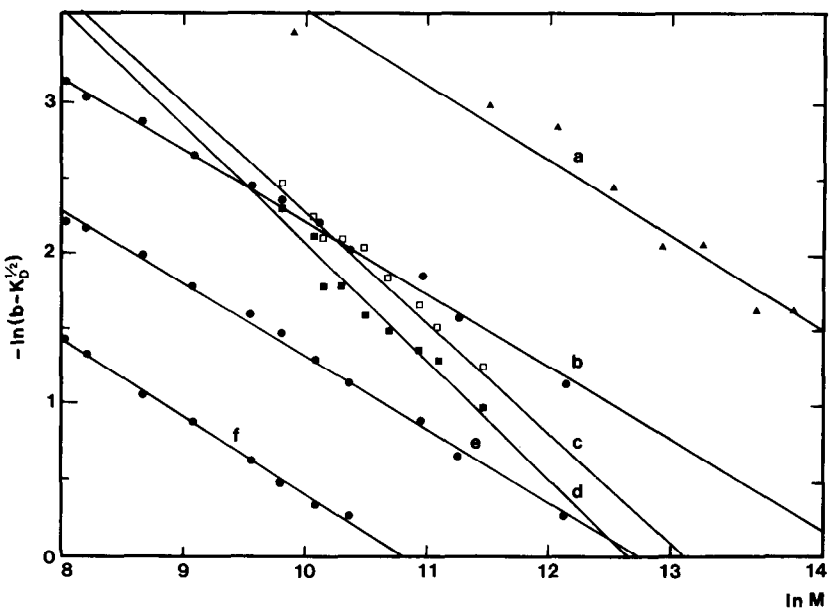

Fig. 2. The GEM plot (eqn. 20) for examples of coils and rods. Polystyrene (▲): (a) R_x 905 (highest M not shown). Dextrans (●): (b) R_x 276; (e) R_x 113; (f) R_x 45. SDS proteins (□): (c) R_x 321; (■): (d) R_x 245. For the remaining five series, cf. Table II.

TABLE II

GEM CORRELATION DATA FOR COILS AND RODS

r = Linear correlation coefficient; N = number of data pairs; $A = A_\theta$ [cm(mol/g)$^{1/2}$] for coils at $T = \theta$; $A = A_0 \mu p^{-m}$ [cm(mol/g)$^{1/3}$] for ellipsoids and rods (*cf.* Table I). In the dextran series the original R_{Hg} values[15] are increased by 5% as indicated by Haller *et al.*[16].

	$R_{H\theta}/10^{-8}$ cm	Eqn. 6: $R_x/10^{-8}$ cm	Eqn. 18: $A_\theta/10^{-8}$	Eqns. 6 and 18		Eqn. 20			N
				b	r	Slope $\lvert x\rvert$	$A/10^{-8}$	r	
Polystyrene	121	112.8	0.1789	1.031	0.993	0.5293	0.1258	0.994	8
	900	904.5	0.1793	1.010	0.991	0.5011	0.1598	0.982	9
Dextran	44.1	45.0	0.1999	1.045	0.997	0.5128	0.1770	0.998	8
	83.5	84.5	0.1999	1.036	0.999	0.5013	0.1972	0.999	10
	119.2	112.6	0.1999	1.044	0.999	0.4861	0.2303	0.998	11
	164.9	173.1	0.1999	1.037	0.998	0.4750	0.2583	0.995	11
	271.4	275.6	0.1998	1.041	0.997	0.4811	0.2428	0.998	11
SDS protein	98.5	82.0	–	0.889	0.977	0.7374	0.0197	0.970	9
	140	145.9	–	0.927	0.990	0.7015	0.0288	0.985	10
	235	245.1	–	1.005	0.987	0.7765	0.0130	0.980	10
	325	320.9	–	1.046	0.995	0.7131	0.0256	0.993	9

[η], were chromatographed by Haller[15,16] on glasses of five different pore radii. The $\bar{M}_w$ values ranged from $287 \cdot 10^3$ to 1000 with $\langle \bar{M}_w/\bar{M}_N \rangle \approx 1.1$. V_0 was measured by TMV elution, and $V_i + V_0$ as the difference between column and CPG volumes. Aqueous glycine buffer (pH 8.2) was used as eluent. The results were given as K_D *vs.* log $\bar{M}_w$ plots only. K_D values were therefore read directly from the figures, whereas R_e was determined as follows.

From the tabulations of Basedow *et al.*[14] we obtain the Mark-Houwink equation $[\eta] = 0.11408\ \bar{M}_z^{0.50016}$ ($r = 0.9988$) where the units of [η] are cm^3/g and $\bar{M}_z$ is a "sedimentation average". Using the theoretical ξ value of 0.875 and $M_0 = 162.18$, this expression was transformed into eqn. 11a, such that

$$R_e = 1.9945 \cdot 10^{-9}\ \bar{M}_z^{0.50016}\ \text{(cm)} \tag{21}$$

Since $\bar{M}_w$ and $\bar{M}_z$ are tabulated, the R_e values could be directly applied to Haller's data. Because ξ will approach unity with decreasing M, data for $\bar{M}_z < 3000$ were not computed. Readings for $K_D < 0.05$ were likewise excluded. The results are illustrated in Figs. 1 and 2 and given in Table II.

SDS-denaturated proteins

Reduced proteins were denatured by SDS and analysed in four different CP glasses by Collins and Haller[17]. V_0 was obtained by the use of TMV and $V_i + V_0$ from tryptophan. A SDS-containing phosphate buffer (pH 7.0) was used as eluent. The results were given in the form of K_D *vs.* log M plots alone. In order to evaluate R_e we used the log R_η : log M correlation for reduced proteins associated with 1.4

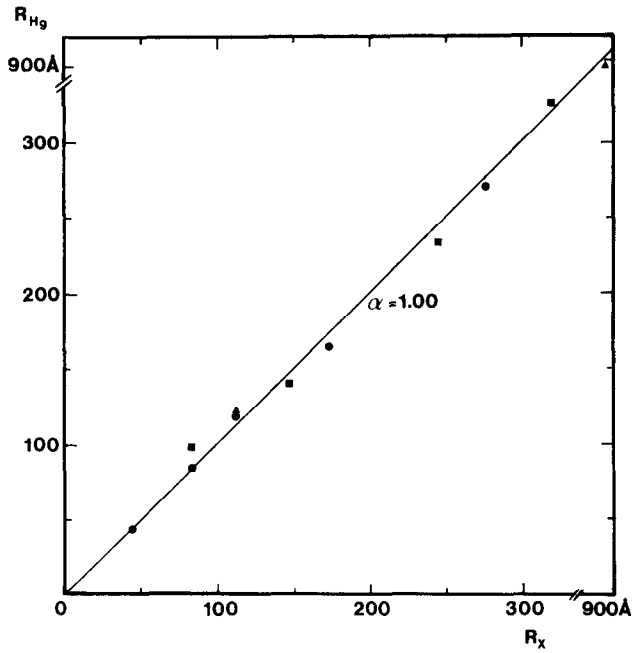

Fig. 3. Comparison of calculated and directly measured pore radii for eleven glasses. R_x from eqn. 6, R_{Hg} from intrusion porosimetry. Data points: ▲ = polystyrenes; ● = dextrans; ■ = SDS proteins.

g of SDS per gram of protein given by Fish *et al.*[18], which for the range of M 17 000 to 70 000 yields

$$R_\eta \simeq 0.2455 \cdot 10^{-9}\, M^{0.73} \text{ (cm)} \tag{22}$$

A χ value of 0.87, originally chosen[2] to convert R_η into R_e and employed in this paper, will be discussed below. Since the above $R_\eta : M$ correlation is not valid for $M < 17\,000$ and has not been worked out for high values, the data treatment was limited to ten proteins in the range $17\,000 < M < 100\,000$. Results are shown in Fig. 2, and given in Table II.

RESULTS AND DISCUSSION

Pore size and shape

The data compiled in Table II appear to corroborate fully the basic assumptions expressed by eqns. 6 and 7. Thus, the agreement between measured and calculated pore radii, illustrated in Fig. 3, is given by $\langle R_{Hg}/R_x \rangle = 1.015 \pm 0.073$ ($N = 11$) or 0.996 ± 0.041 ($N = 10$). Moreover, the predicted linearity of $K_D^{\frac{1}{2}}$ *vs.* R_e is borne out by $\langle r \rangle = 0.993 \pm 0.007$.*

In all but two cases the intercept $b > 1.00$, as expected. The lowest b and r

* Since eqns. 6 and 18 for coils yield identical y-intercepts and correlation coefficients, only plots for eqn. 18 are depicted here (*cf.* Fig. 1). $K_D^{\frac{1}{2}}$ *vs.* R_e plots for rods appear in ref. 2, with K_{AV} replacing K_D.

correspond and give the highest deviation from unity for R_{Hg}/R_x, indicating an increased experimental error margin. Specific adsorption effects, described elsewhere[11], would obviously also influence the results.

The radius δ of the postulated diffusion layer (eqns. 2–6) is calculated from $\delta = (b - 1)R_x$ to $6.2 \pm 4.6 \cdot 10^{-8}$ cm and seen to increase with R_x. The degree of increase varies for the three sets of data, probably owing to the different V_i and V_0 determinations. Experiments specifically aimed at elucidating this question and done under conditions where no adsorption takes place remain to be performed.

It is relevant to compare our results with the partition coefficients for random coils in pores of various shapes calculated from equilibrium thermodynamics by Casassa[5] and Casassa and Tagami[1]. This is done in Fig. 4. By the use of the same polystyrene experiments[13] as analysed here, they found the data to lie close to their theoretical curve for slabs, *i.e.* lamellar voids. The reason for this result, considered as improbable by the authors themselves, is the use of the gyration radius R_G instead of R_e. In fact, the two heaviest fractions would simply have been excluded from the R_{Hg} 121-glass if R_G were the decisive parameter. By employing $R_e \simeq 0.665\ R_G$ (eqn. 10a), their curve for cylindrical pores is approached. However, as clearly apparent from Fig. 4, the experimental data actually coincide far better with the theoretical curves for cylinders calculated from the GEM eqn. 6 for two intercept values.

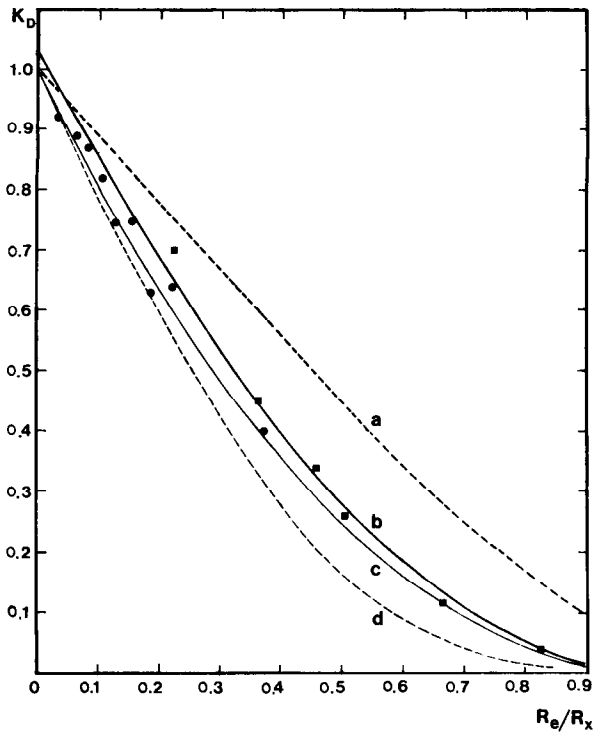

Fig. 4. Casassa's theory (CT)[5] compared with the geometrical exclusion model: (a) CT for slabs; (b) eqn. 6 (b = 1.03); (c) eqn. 6 (b = 1.00); (d) CT for cylindrical pores. Data for polystyrenes[13] in R_x 905 (●) and R_x 113 (■) (*cf.* Table II). With $R_G \simeq 1.5\ R_e$, all data points lie close to curve a.

Molecular structure

The extension of eqn. 6 to molecular weights of random coils in ideal solvents (eqn. 18) is illustrated in Fig. 1, and the logarithmic GEM plot, applicable to all substances, is shown in Fig. 2 for coils and rods in six different glasses. It is noted from Table II that eqn. 18 generally gives the best linear correlation. The reason is that a 10% error in K_D is reflected as $\approx$ 5% in $K_D^{\frac{1}{3}}$, but increases with K_D in the logarithmic term to $\approx$ 80% for K_D 0.90. Moreover, the inherent weakness of the eqn. 20 plot is the sensitivity of the slope to b. This might be solved by equilibrium measurements of V_i from which $b = 1.00$ and R_x becomes slightly greater than R_{Hg}.

In spite of these factors, an average dextran slope of 0.491 $\pm$ 0.015 is obtained from eqn. 20 (*cf.* Table II) and seen as a satisfactory result. Under conditions of non-ideality the expansion factor α can be calculated from this plot if the bond length β is known. In all cases, the required R_x may be determined once for all or replaced by the manufacturer's R_{Hg} for narrow pore distributions, whereas the monomer weight M_0 is known. For ideality ($\alpha = 1.00$), β is then directly calculated from the intercept (eqn. 20) or the slope (eqn. 18). Thus, the following values for $\beta/10^{-8}$ cm are found (*cf.* Table II):

	Eqn. 18	Eqn. 20
Polystyrene	4.76	4.26 (R_{Hg}900)
Dextran	9.38	10.38 $\pm$ 1.6

as compared with 4.96 (307 K) and 4.86 (light scattering) for polystyrene[8], and 11.2–8.2 for Dextran B 512-Ph calculated from Granath's results[19].

For coils in any solvent, eqn. 20 plots provide the data required to calculate the gyration radius R_G from eqn. 9. From the same plots, the diffusion coefficient D^0 for any chemical species is readily determined by replacing $R_e = A M^x$ into eqn. 4.

The analysis of rods is more complicated, because the original results were given in R_η, which we had to convert into R_e. A constant factor of $\chi = R_e/R_\eta = 0.87$ was applied. The average slope of 0.732 $\pm$ 0.03 and A_0 of 0.0218 $\pm$ 0.007 $\cdot 10^{-8}$ cm determined by the GEM plot agree perfectly with the parameters in eqn. 22. However, a constant χ for rods is in evident contradiction with the fact that χ is a function of a/b as given by eqn. 17. On the other hand, the axial ratios are not known. Since we have shown that R_η varies with $M^{(1+m')/3}$, and $\nu = \mu'(a/b)^{m'}$, from $M^{0.73}$ one finds $m' = 1.19$, which corresponds to a range of $\approx 4 \leqslant (a/b) \leqslant 12$, equivalent to χ 0.960 $-$ 0.857 or an average some 4% higher than the value employed. The fact that the slope from eqn. 20 is identical with the exponent of M in eqn. 22, may indicate that the use of a constant χ is compensated by the experimental error. A detailed analysis of this question is forthcoming[11].

One of the fundamental conclusions is the fact that the slope of the logarithmic GEM plot allows the immediate recognition of the type of structure. Thus, the following approximate limits can be evaluated:

	Slope $\|x\|$ (eqn. 20)
Rod-like molecules	0.63–$\approx$ 0.8
Random coiled polymers, $T = \theta$	0.50
Random coiled polymers, $T \neq \theta$	$>$0.5–$\approx$ 0.6
Globular proteins[11] (prolates)	0.37–0.39

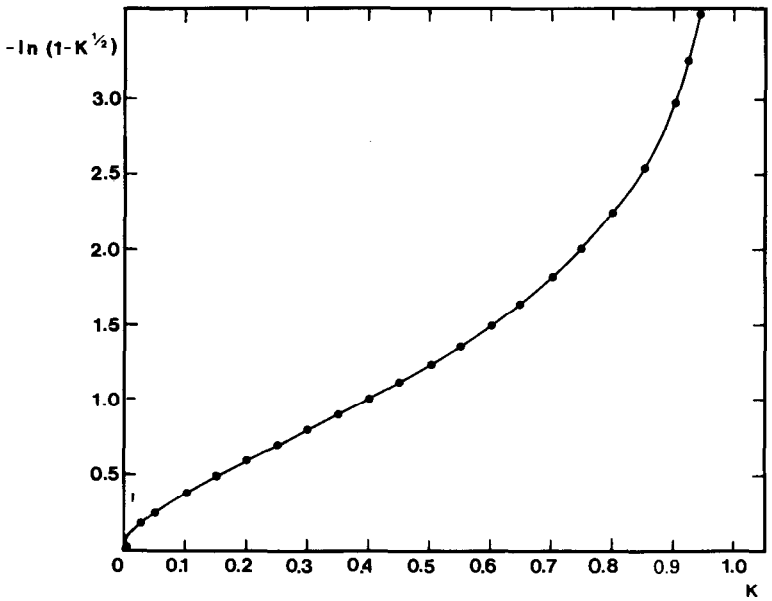

Fig. 5. Generation of the empirical K: log M curve by correlating $-\ln(1 - K^{\frac{1}{2}})$ (eqn. 20) with K (see text).

Polymer branching is expected to lead to lower values. The slope for rods is practically constant for axial ratios above $\approx$ 25–30. At lower values the slope and therefore the linearity of the logarithmic plot decreases with decreasing a/b.

In all cases, the exclusion value for M is given by $M_{ex} = (b\ R_x/A)^{1/x}$ where $1/x = 2$ for eqn. 18.

Linear expressions have obvious advantages in column calibration, especially when a number of parameters are known beforehand. This is in clear contrast to the widely used, empirical, K_D *vs.* log M correlations. Their sigmoidal shape and characteristic quasi-linear portion are seen in Fig. 5, in which $-\ln(1 - K^{\frac{1}{2}})$ is plotted against K. The substantial linear part extends from K 0.05 to 0.55 and has a correlation coefficient of $r = 0.9995$. At higher K values the curvature increases and subsequent quasi-linear ranges become much narrower. The actual shape of a K_D *vs.* log M curve will therefore exclusively depend on the range covered. Its slope is negative and approaches zero for $K_D \rightarrow 1.0$ and $K_D \rightarrow 0$. No physical rationale for these plots appears to have been given previously.

REFERENCES

1 E. F. Casassa and Y. Tagami, *Macromolecules*, 2 (1969) 14.
2 H. Waldmann-Meyer, in R. Epton (Editor), *Chromatography of Synthetic and Biological Polymers*, Vol. 1, Ellis Horwood, Chichester, 1978, Ch. 19, p. 289.
3 H. Waldmann-Meyer, in A. Frigerio and H. Milon (Editors), *Chromatography and Mass Spectrometry in Nutrition Science and Food Safety*, Elsevier, Amsterdam, 1984, p. 257.
4 H. Waldmann-Meyer, *Abstracts 8th International Biophysics Congress, Bristol, 1984*, Nr. 157.
5 E. F. Casassa, *J. Polym. Sci., Part B*, 5 (1967) 773.
6 W. Haller, *Nature (London)*, 206 (1965) 693.
7 W. Haller, *J. Chem. Phys.*, 42 (1965) 686.

8 Ch. Tanford, *Physical Chemistry of Macromolecules*, Wiley, New York, 1961.
9 E. G. Richards, *An Introduction to Physical Properties of Large Molecules in Solution*, Cambridge University Press, New York, 1980.
10 Ch. R. Cantor and P. R. Schimmel, *Biophysical Chemistry, Part II*, Freeman, San Francisco, CA, 1980.
11 H. Waldmann-Meyer, in preparation.
12 H. Bénoit, Z. Grubisic, P. Rempp, D. Decker and J. G. Zilliox, *J. Chim. Phys.*, 63 (1966) 1507.
13 J. C. Moore and M. C. Arrington, *International Symposium on Macromolecular Chemistry, Tokyo-Kyoto, 1966*, Preprints, VI-107.
14 A. M. Basedow, K. H. Ebert, H. Ederer and H. Hunger, *Makromol. Chem.*, 177 (1976) 1501.
15 W. Haller, *Macromolecules*, 10 (1977) 83.
16 W. Haller, A. M. Basedow and B. König, *J. Chromatogr.*, 132 (1977) 387.
17 R. C. Collins and W. Haller, *Anal. Biochem.*, 54 (1973) 47.
18 W. W. Fish, J. A. Reynolds and Ch. Tanford, *J. Biol. Chem.*, 245 (1970) 5166.
19 K. A. Granath, *J. Colloid Sci.*, 13 (1958) 308.